Plasmonics (2023) 18:711–717
https://doi.org/10.1007/s11468-023-01800-5

The Band Gap of Silver Nanoparticles in Ag/Ag_2O Composites Synthesized by Oxygen Plasma Treatment of Silver Thin Films

Kamal Kayed[1] · Mayada Issa[2] · Esaaf Alsoki[3]

Received: 12 January 2023 / Accepted: 7 February 2023 / Published online: 13 February 2023

Abstract
In this paper, we explore the band gap properties of Ag/Ag_2O composites synthesized by oxygen plasma treatment of silver thin films as well as the band gap properties of silver nanostructures formed within these composites. The band gap of silver nanoparticles was calculated based on a previous unique result including that the luminescence spectra of the prepared Ag/Ag_2O composites contain only features that characterize the various structures of silver nanoparticles. The results obtained showed the formation of energy bands of silver nanoparticles within the energy band structure of the prepared films. Based on the observed features of the luminescence spectra, distinguished energy gaps were found for both individual silver nanoparticles and larger silver nanoparticles. Moreover, the energy gap of individual silver nanoparticles is not significantly affected by neither the size of the silver oxide particles nor the power of the oxygen plasma.

Keywords Silver oxide · Optical transmission spectra · Luminescence spectra · Silver nanoparticles · Thermal evaporation · Band gap · Oxygen plasma afterglow

Introduction

The doping of various solid materials with silver nanoparticles is highly beneficial in many fields comprising applications in optoelectronics, solar cells, surface chromatography optics, imaging, photocatalysis, surface-enhanced Raman scattering, data storage media, etc. [1–8]. Conversely, the employment of surface plasmons of materials doped with silver nanoparticles requires examining the interactions between these particles, along with investigating the effect of their size, shape, and the nature of the dielectric material on the response of surface plasmons [9–18].

In our previous work [19], silver thin films were synthesized by thermal evaporation of silver samples. Then, the silver films were exposed to oxygen plasma currents at various powers. The optical absorbance spectra of the prepared samples were analyzed. The results show that the plasmon power has significant effects on the properties of the plasmon resonance peaks (position, spectral width, and intensity). On the contrary, a slight degradation was observed in the individual plasmon peaks of the silver nanoparticles. It has been suggested that this decomposition occurs due to the mutual interaction between individual silver nanoparticles located near the shell of Ag_2O grains and larger nanoparticles located in neighboring grains. The results also showed that the degree of decomposition is related to the size of the silver oxide (Ag_2O) particles. On the other hand, we found in another work [20] that the individual silver nanoparticle peak degradation observed in the optical absorption spectra has a mirror image in the photoluminescence spectra. In addition, the results showed that this degradation arises due to the mutual interaction between the individual silver nanoparticles located near the Ag_2O grain shell and the larger silver nanoparticles inside the grain, and it is related to the silver oxide grain size [20].

A previous study [21] dealing with the optical properties of silver nanoparticles showed that these particles possess a direct band gap of 2.51 eV. It is found that the band gap of silver nanoparticle-doped materials depends on the size and shape of the nanoparticles. The model predicts that the

✉ Kamal Kayed
khmk2000@gmail.com;
kamal.kayed2@damascusuniversity.edu.sy

[1] Department of Physics, Faculty of Science, Damascus University, Damascus, Syria

[2] Department of Chemistry, Faculty of Science, Damascus University, Damascus, Syria

[3] College of Engineering and Technology, American University of the Middle East, Ahmadi, Kuwait

band gap increases with decreasing nanoparticle size of the semiconductor material [1, 12, 22, 23]. On decreasing the size, the electron gets confined to the particle (confinement effects) leading to increase in band gap. With reducing size of the particle, the density of states becomes more quantized, and the band gap shifts to higher energies (shorter wavelengths) [4, 24]. In this article, we employ the unique optical and structural properties of Ag/Ag_2O composites in order to demonstrate the formation of energy bands of silver nanoparticles and investigate their influence on the band gap properties of silver oxide films.

Experimental

Sample Preparation

Thin films of silver with a thickness of 316 nm were deposited at air temperature on silicon and glass substrates by thermal evaporation of silver targets using the JSM200 system. Technical details of the sedimentation processes using the thermal evaporation system can be found in our previous works [25–27]. The prepared silver films were subjected to reactive oxygen plasma afterglow (OPA) at a certain plasma power in order to obtain the compositions. Molecular oxygen plasma was generated using a SAIREM GMP 20 KEDS microwave with various powers in the range of 250–1250 W. Table 1 shows the plasma capacity for each of the treated samples.

More details about the plasma generation system are explained in previous works [25–27].

Sample Characterization

Crystallite structure of the films was measured by X-ray diffraction (XRD) using (Stoe StadiP) transmission X-ray diffractometer employing a Cu $K\alpha_1$ ($\lambda = 1.54060$ Å) source. The optical transmittance and absorption spectra were recorded with a UV–vis spectrophotometer (Cary 5000). The photoluminescence (PL) spectra were recorded at room temperature using a He–Cd laser with an excitation wavelength of 325 nm. A grating monochromator (1200 groves/mm) and cooled photomultiplier tube PMT were also used to measure PL spectra.

Table 1 The plasma capacity for each of the treated samples

Sample label	Plasma power
A	250.00 W
B	500.00 W
C	750.00 W
D	1000.00 W
E	1250.00 W

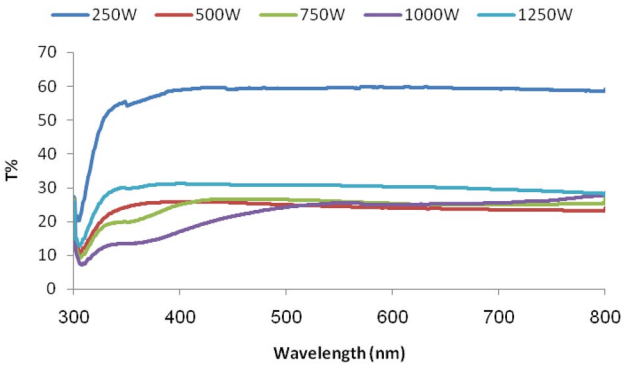

Fig. 1 The optical transmission spectra of the prepared Ag_2O thin films

Results and Discussion

The optical transmission spectra of the oxygen plasma-treated silver thin films are shown in Fig. 1. We notice that, outside the surface plasmon absorption region ($\lambda > 500$ nm), the optical transmission is almost equal for all oxygen-rich films (samples: B, C, and D), with a value of about 28%. On the contrary, the samples with metallic structure (samples A and E) have higher transmission. Sample A is more transparent than sample E because of its higher porosity [19]. In the region ($\lambda < 500$ nm), spectra spacing of oxygen-rich samples as a result of appearance of plasmon absorption bands can be observed. The formation of these bands contributes to making transmission more sensitive to the oxygen content in the film.

Optical transmittance spectra were used to calculate the band gap (Tauc gap) for all samples. The band gap is calculated from Davis and Mott equation [4, 28, 29]:

$$\alpha h\upsilon = A(h\upsilon - Eg)^{0.5} \quad (1)$$

where $h\upsilon$ is the energy of the incident light, E_g is the estimate of the band gap, and A is a constant. Therefore, E_g can be found by plotting the variation of $(\alpha h\upsilon)^2$ against $h\upsilon$, where the extrapolation of the linear region of the curve with X-axis gives the value of band gap of thin film. Figure 2

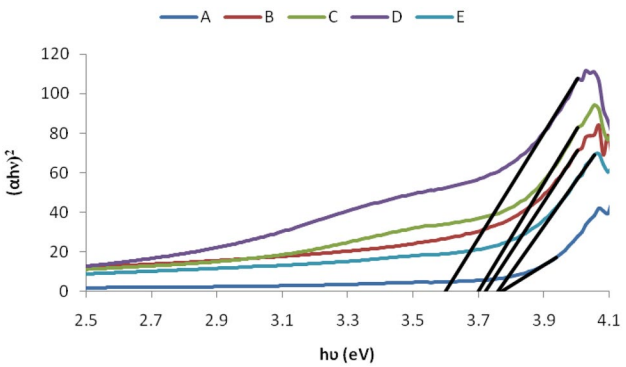

Fig. 2 $(\alpha h\upsilon)^2$ as a function of $h\upsilon$ for all samples

Table 2 The band gap values of Ag/Ag_2O composites and all silver nanostructures

Eg (eV)						
Sample label	**Ag/Ag_2O composites**	**Total Ag NPs**	**L Ag NPs**	**I Ag NPs**	**I Ag NPs (1)**	**I Ag NPs (2)**
A	3.770	2.436	2.386	2.855	2.796	2.886
B	3.722	2.872	2.543	2.855	2.776	2.890
C	3.700	2.837	2.557	2.837	2.768	2.882
D	3.599	2.449	2.398	2.872	2.828	2.903
E	3.759	2.281	2.205	2.837	2.844	2.845

shows the method of calculating of the band gap for all samples. The band gap values for all samples (Ag/Ag_2O composites) are listed in Table 2.

In our previous work [20, we found that the luminescence spectra of our samples (Fig. 3) do not have features specific to silver oxide and that all features appearing in these spectra are due to silver nanoclusters. We found that each of these spectra can be deconvoluted into two main peaks, the "I" peak and the "L" peak. The "I" peak is due to the presence of individual silver nanoparticles, while the "L" peak is due to the presence of larger silver nanoparticles.

Figure 4 shows an example of the PL spectrum deconvolution process that concerns the spectrum of sample D that was treated at 1000 W.

We also found that peak I results from the summation of two sub-peaks, peak 1 resulting from individual silver nanoparticles located within the silver oxide grain and peak 2 resulting from individual silver nanoparticles located near the grain shell. Figure 5 shows the peaks "1" and "2" resulting from the deconvolution process of the "I" peak in the PL spectrum of the sample C that was treated at 500 W [20].

The important result of our previous work [20] is that each of the peaks that appeared in the fluorescence spectra has a mirror image in the optical absorption spectra.

It is known in the PL spectra that the position of the peak indicates the value of the band gap [24]. Accordingly, we have included in Table 2 the band gap values for the following components: total silver nanoparticles (total Ag NPs), individual silver nanoparticles (I Ag NPs), larger size silver nanoparticles (L Ag NPs), individual silver nanoparticles located within the grain (I Ag NPs (1)), and individual silver nanoparticles located near the grain shell (I Ag NPs (2)). The band gap of silver nanoparticles (total Ag NPs) can be observed in Fig. 2, especially in the curves of both C and D samples, where a broad shoulder is formed in the range from 3.2 to 3.6 eV.

Figure 6 shows the band gap of Ag/Ag_2O composites and total silver nanoparticles (total Ag NPs) as a function of plasma power.

It has been observed in the composites of Ag/Ag_2O that the band gap decreases slightly with the increase in the plasma power, but it returns to increase when $W = 1250$ W (sample E) due to a decrease in the rate of the silver oxidation reaction [19]. The essential outcome is drawn clearly in this figure showing that the formation of silver nanoparticles leads to the formation of energy bands belonging to these

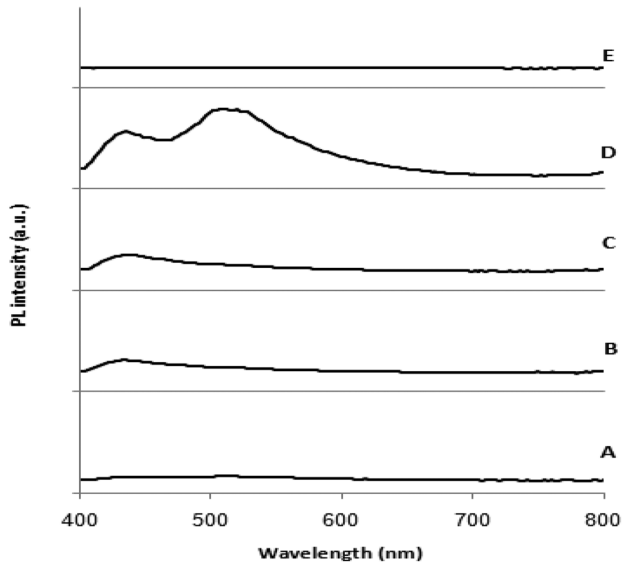

Fig. 3 The luminescence spectra of the prepared samples

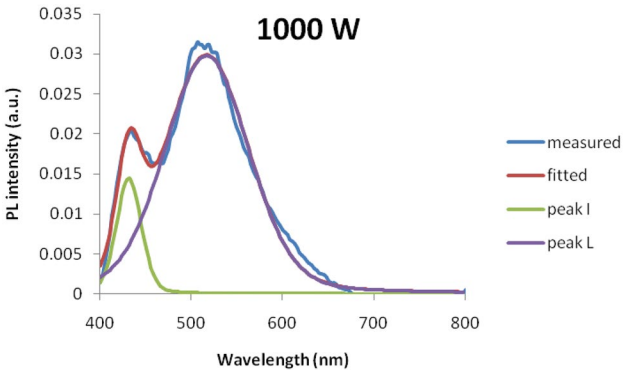

Fig. 4 The deconvoluted PL spectrum of the sample D

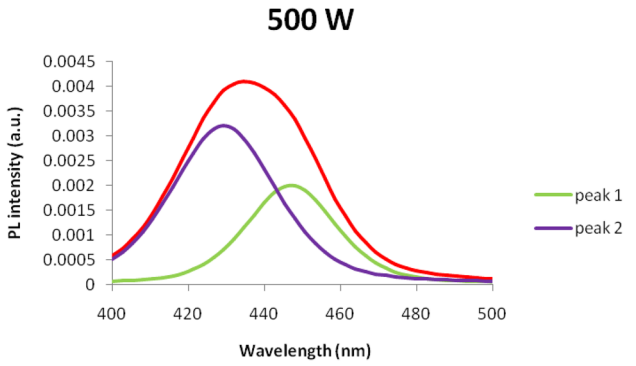

Fig. 5 Peaks "1" and "2" resulting from the deconvolution process of the "I" peak in the PL spectrum of the sample C

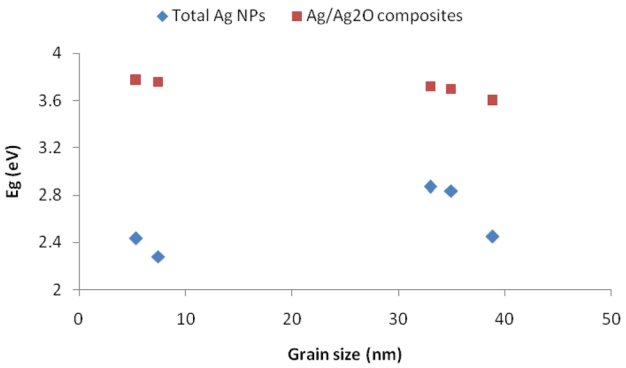

Fig. 7 The band gap of Ag/Ag_2O composites and total silver nanoparticles (total Ag NPs) as a function of Ag_2O grain size

particles within the band gap of each sample. Moreover, it has been found that the band gap of the silver nanoparticles (total Ag NPs) is more affected by the plasma power. It exhibits a unique behavior that alternates between increasing and decreasing, resulting in maxima for the band gap in the region at 500–750 W.

It has been found in our previous work [19] that the plasma power affects the grain size, so in order to disprove the behavior of the band gap in Fig. 6, we investigated the relationship between the band gap and the silver oxide grain size (Fig. 7).

The effect of size on the band gap is clearly visible in the case of the Ag/Ag_2O composites where the band gap decreases with the increase of the silver oxide grain size; this is consistent with the results of quantitative studies of the properties of nanomaterials [24]. On the other hand, it seems that the effect of the size is also present in the case of the total silver nanoparticles (total Ag NPs), especially in the case of samples rich in oxygen (samples B, C, and D). The points close to the coordinate principle are for samples with low oxygen content (samples A and E). It is clear from the figure that these samples have their own size effect as the band gap decreases with the increase of the grain size according to a special approach that differs from that of the rest of the samples.

Figure 8 shows the band gap of silver nanoparticles (total Ag NPs, I Ag NPs, and L Ag NPs) as a function of plasma power. It appears from this figure that the band gap of I Ag NPs is not significantly affected by the plasma power, while larger nanoparticles which have a lower band gap are greatly affected by the plasma power, and it behaves similar to the behavior of the total Ag NPs.

On the other hand, the distance from the curve of the total nanoparticles (bold line) can be used to estimate the density of silver nanoparticles. In the case of oxygen-rich samples (samples B and C), the density of individual nanoparticles is higher due to their proximity to the solid curve, while in other samples, the density of larger nanoparticles is higher.

Figure 9 illustrates the relationship between the band gap of silver oxide nanoparticles (total Ag NPs, I Ag NPs, and L Ag NPs) and the silver oxide grain size.

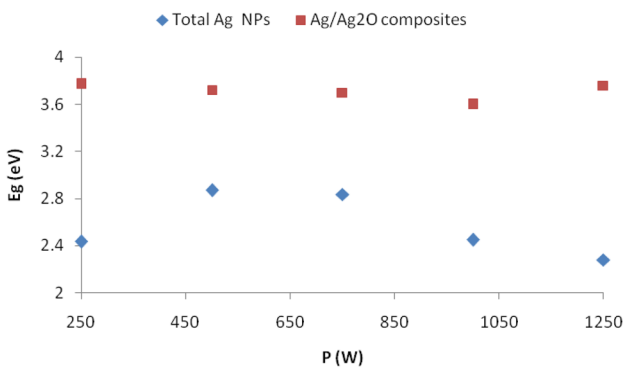

Fig. 6 The band gap of Ag/Ag_2O composites and total silver nanoparticles (total Ag NPs) as a function of plasma power

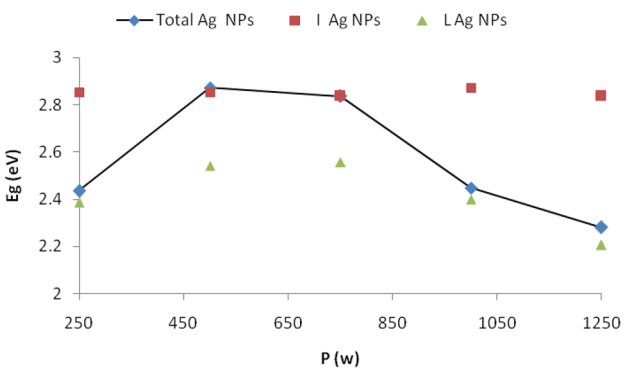

Fig. 8 The band gap of silver nanoparticles (total Ag NPs, I Ag NPs, and L Ag NPs) as a function of plasma power

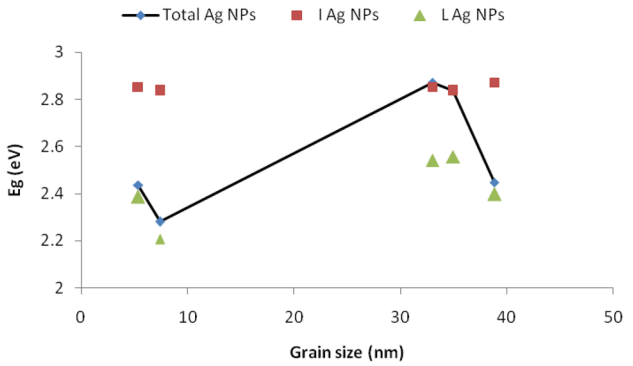

Fig. 9 The band gap of silver nanoparticles (total Ag NPs, I Ag NPs, and L Ag NPs) as a function of silver oxide grain size

This figure shows that the band gap of I Ag NPs is not significantly affected by the silver oxide grain size, while larger nanoparticles which have a lower band gap are greatly affected by the silver oxide grain size, and it behaves similar to the behavior of the total Ag NPs.

Figure 10 shows the relationship between the band gap of silver oxide nanoparticles (I Ag NPs (1) and I Ag NPs (2)) and the silver oxide grain size.

In general, the band gap of individual silver nanoparticles near the shell of a silver oxide grain (I Ag NPs (2)) is wider than that of individual silver nanoparticles located inside the grain (I Ag NPs (1)).

The absorption spectra of our samples [19] previously revealed that the ratio p_2/p_1 (which is the relative intensity of the I Ag NPs (2) peak and I Ag NPs (2)) is related to the oxide particle size (x) through the relationship:

$$p_2/p_1 = \alpha - \beta.x^2 \tag{2}$$

where $\alpha = (4.652)$ and $\beta = (0.0001)$.

This relationship excludes the sample (A) and indicates the decrease of the ratio p_2/p_1 as the grain size increases.

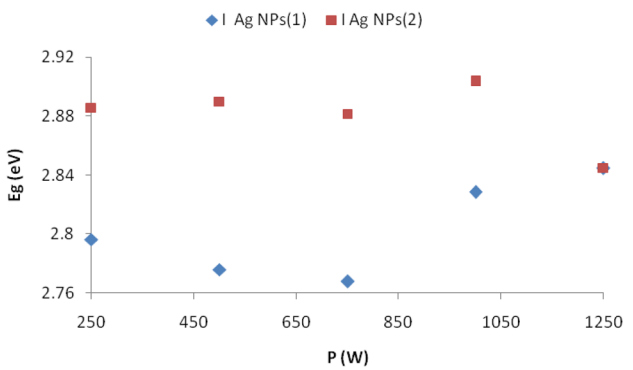

Fig. 10 The band gap of silver oxide nanoparticles (I Ag NPs (1) and I Ag NPs (2)) as function of plasma power

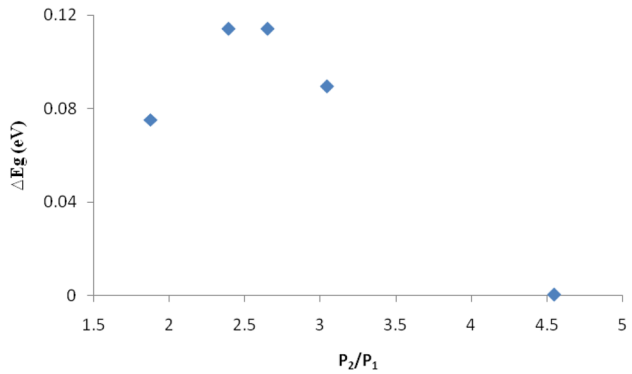

Fig. 11 ΔEg as a function of the ratio p_2/p_1

The p_2/p_1 ratio is a measure of the degree of degradation of the optical absorption peak of individual silver nanoparticles [19]; therefore, it can be useful to investigate its relationship with ΔEg (Fig. 11), where:

$$\Delta Eg = Eg_{(\mathrm{IAgNPs(2)})} - Eg_{(\mathrm{IAgNPs(1)})} \tag{3}$$

Moreover, Fig. 11 shows how the curve goes through two phases, increasing and decreasing, and it reaches its maximum in the range of 2.39–2.65 on the p_2/p_1 axis. It has also shown the point behavior from left to right according to the decrease in oxygen content, except for the last point of sample E, which has a higher oxygen content than sample A in spite of having a porous structure [19].

In our previous work [19], we found that the super-soft structure is obtained when $p_2/p_1 = 4.652$. In Fig. 11, this value is close to the point of intersection of the curve with the p_2/p_1 axis, and it corresponds to a zero value of ΔEg. However, the intersection point with the axis of ΔEg corresponds to the state of non-degradation, which is the disappearance of the peak p_2, where $p_2/p_1 = 0$.

Conclusions

In this work, we subjected thin silver films deposited on silicon and glass substrates by thermal evaporation method to oxygen plasma streams of various powers in order to obtain Ag/Ag_2O composites. The optical properties (luminescence and transmission spectra) of the prepared samples were investigated. The data of the optical property study were linked with the data of the structural analysis in order to give an integrated description of the band gap for each of the Ag/Ag_2O composites and silver nanoparticles. Unique results were obtained and summarized as follows:

1. The energy gap of the Ag/Ag_2O composites decreases with the increase of silver oxide grain size.

2. Formation of energy bands of silver nanoparticles within the energy band structure of the Ag/Ag_2O composites has been observed.
3. The energy gaps of the individual silver nanoparticles were distinguished from those of the larger silver nanoparticles.
4. The impact of size on the energy gap is evident for both the total silver nanoparticles (total Ag NPs) and the larger silver nanoparticles (L Ag NPs).
5. The energy gap of the individual silver nanoparticles (total Ag NPs) is not significantly affected by neither the size of the silver oxide particles nor the power of the oxygen plasma.
6. Silver nanoparticles within the silver oxide grains have a wider band gap compared to those near the grain shell.
7. For the super-soft structure, the band gap of silver nanoparticles within the grain is equivalent to those near the shell.

Acknowledgements The authors would like to thank the University of Damascus and the Syrian Atomic Energy Commission for providing the facility to carry out this research. They would also like to thank Dr. A. Alkhawwam for the assistance during working on the Microwave SAIREM GMP 20 KEDS system.

Author Contribution All authors had equal percentages of work completion.

Availability of Data and Materials Not applicable.

Declarations

Ethical Approval This is an observational study. No ethical approval is required.

Consent to Participate Not applicable.

Consent for Publication Not applicable.

Conflict of Interest The authors declare no competing interests.

References

1. Sun W, Hong R, Liu Q, Li Z, Shi J, Tao C, Zhang D (2019) SERS-active Ag–Al alloy nanoparticles with tunable surface plasmon resonance induced by laser ablation. Opt Mater 96:109298
2. Dubas ST, Pimpan V (2008) Green synthesis of silver nanoparticles for ammonia sensing. Talanta 76:29–33
3. Biswanath M, Moumita M (2009) Nonvolatile memory device based on Ag nanoparticle: characteristics improvement. Appl Phys Lett 94:233–236
4. Chiyah B, Kayed K (2018) Effect of annealing temperature on the structural and optical properties of silver oxide thin films prepared by thermal evaporation with subsequent annealing. Int J Nanoelectron Mater 11:305–310
5. Yang GW, Li H (2008) Sonochemical synthesis of highly monodispersed and sizecontrollable Ag nanoparticles in ethanol solution. Mater Lett 62:2189–2191
6. Li S, Gao B, Wang Y, Jin B, Yue Q, Wang Z (2019) Antibacterial thin film nanocomposite reverse osmosis membrane by doping silver phosphate loaded graphene oxide quantum dots in polyamide layer. Desalination 464:94–104
7. Zhao WB, Zhu JJ, Chen HY (2003) Photochemical synthesis of Au and Ag nanowires on a porous aluminum oxide template. J Cryst Growth 258:176–180
8. Dubas ST, Pimpan V (2008) Humic acid assisted synthesis of silver nanoparticles and its application to herbicide detection. Mater Lett 62:2661–2663
9. Dubas ST (2007) Preparation of silver nanoparticle thin films for sensing application (Ph.D. thesis), Department of Material Science, Chulalongkorn University,Bangkok, Thailand
10. Hossain MK, Drmosh QA (2022) Silver nanoparticles and nanorings for surface-enhanced Raman scattering. Plasmonics 17:1051–1064. https://doi.org/10.1007/s11468-021-01572-w
11. Huang LM, Wen TC (2007) One-step synthesis of silver nanoparticles and poly(2,5-dimethoxyaniline) in poly(styrene sulfonic acid). Mater Sci Eng A445–446:7–13
12. Filippo E, Serra A, Manno D (2009) Poly(vinyl alcohol) capped silver nanoparticles as localized surface plasmon resonance-based hydrogen peroxide sensor. Sens Actuators B Chem 138:625–630
13. Ling L, Feng Y, Li H, Chen Y, Wen J, Zhu J, Bian Z (2019) Microwave induced surface enhanced pollutant adsorption and photocatalytic degradation on Ag/TiO2. Appl Surf Sci 483:772–778
14. Mahapatra SS, Karak N (2008) Silver nanoparticle in hyperbranched polyamine: synthesis, characterization and antibacterial activity. Mater Chem Phys 112:1114–1119
15. Wadayama H, Okabe T, Taniguchi J (2018) Fabrication of multilayered structure of silver nanorod arrays for plasmon memory. Microelectron Eng 193:47–53
16. Li M, Wang Y, Xing Y, Zhong J (2020) P123-assisted preparation of Ag/Ag2O with significantly enhanced photocatalytic performance. Solid State Sci 99:106062
17. Uğur Ş, Akaoğlu C, Kucukkahveci E (2019) A study on film formation and fluorescence enhancement of PS latex/AgNPs composites depending on AgNPs content and annealing. Colloids Surf A 573:40–56
18. Ren J, Tilley RD (2007) Preparation, self-assembly, and mechanistic study of highly monodispersed nanocubes. J Am Chem Soc 129:3287–3291
19. Kayed K (2020) The optical properties of individual silver nanoparticles in Ag/Ag_2O composites synthesized by oxygen plasma treatment of silver thin films. Plasmonics. https://doi.org/10.1007/s11468-020-01169-9
20. Kayed K (2021) The luminescence properties of individual silver nanoparticles in Ag/Ag2O composites synthesized by oxygen plasma treatment of silver thin films. J Lumin 237:118163
21. Aziz A, Khalid M, Akhtar MS, Nadeem M, Gilani ZA, Asghar HMNUHK, Rehman J, Ullah Z, Saleem M (2018) Structural, morphological and optical investigations of silver nanoparticles synthesized by sol-gel autocombustion method. Dig J Nanomater Biostruct 13(3):679–683
22. Abdullah BJ (2022) Size effect of band gap in semiconductor nanocrystals and nanostructures from density functional theory within HSE06. Mater Sci Semicond Process 137:106214
23. Singh M, Goyal M, Devlal K (2018) Size and shape effects on the band gap of semiconductor compound nanomaterials. J Taibah Univ Sci 12(4):470–475. https://doi.org/10.1080/16583655.2018.1473946
24. Smith AM, Nie S (2010) Semiconductor nanocrystals: structure, properties, and band gap engineering. Acc Chem Res 43:190–200

25. Alkhawwam A, Abdallaha B, Kayed K, Alshoufi K (2011) Effect of nitrogen plasma afterglow on amorphous carbon nitride thin films deposited by laser ablation. Acta Phys Pol A 120:545–551
26. Kayed K (2010) Synthesis and properties of carbon nitride and boron nitride thin films prepared by different techniques. Damascus University Syria, Damascus, PhD thesis
27. Kayed K (2018) Effect of nitrogen plasma afterglow on the (1000–1800) cm−1 band in FTIR spectra of amorphous carbon nitride thin films. Spectrochim Acta A Mol Biomol Spectrosc 190:253–258
28. Mott NF, Davis EA (1971) Electronic properties in non-crystalline materials. Oxford University Press, London
29. Wang T, Liu Y, Fang Q, Wu M, Sun X, Lu F (2011) Low temperature synthesis wide optical band gap Al and (Al, Na) co-doped ZnO thin films. Appl Surf Sci 257:2341–2345